STRENGTH AND DUCTILITY PREDICTION OF CONCRETE BEAMS REINFORCED WITH INTERNAL STEEL AND EXTERNAL COMPOSITE MATERIALS

W. Karunasena and W. C. Anderson

Civil & Environmental Engineering, School of Engineering, James Cook University, Townsville, Queensland 4810, Australia

ABSTRACT

Reinforced concrete structures undergo continuous deterioration throughout their service life, and many are required to support loads exceeding initial design loads. Such structures need to be replaced or rehabilitated, with rehabilitation being the cheapest alternative. There are currently a number of techniques available for rehabilitating structural members in functionally obsolete or structurally deficient structures. One such rehabilitation method, getting particular attention during the last decade, is the use of externally bonded fibre reinforced polymers strips to increase or restore load capacity of structurally deficient or functionally obsolete beam, column and slab members. To design for beam rehabilitation, it is fundamentally important that the expected increase in capacity due to the fibre reinforced polymer strip is quantified. In this paper, a simple computational model that predicts the linear and nonlinear behaviour of a fibre reinforced polymer rehabilitated reinforced beam is presented. The model has been implemented in Matrix Laboratory software package. The model quantifies the moment-curvature and load-deflection relationships. The model is verified by comparing numerical results with experimental data for fibre reinforced polymer rehabilitated beams. The results of a parametric study investigating the influence of tensile steel reinforcement and composite reinforcement (carbon or glass fibres) are presented.

1.   INTRODUCTION

FRP composites have been employed for rehabilitation of concrete elements in civil infrastructure for approximately fifteen years. Development of this technology can be attributed to the large number of concrete elements which are structurally deficient due to aging or elements that are required to support loads in excess of their original design loads. This situation is common, particularly in highway bridges. According to Tavakkolizadeh and Saadatnamesh[1], the number of substandard highway bridges in United States alone is 167,000, more than half of which are structurally deficient. Rehabilitation of concrete beams with fibre reinforced polymers (FRP) is becoming an increasingly popular rehabilitation method. This technology started developing after some revolutionary research at the Swiss Federal Laboratory for Materials and Testing Research[2]. Desirable characteristics of FRP laminates, in the context of concrete element rehabilitation, include: high strength-to-weight ratio, high directional strength, light weight, corrosion resistance, high impact strength and low maintenance. Rehabilitation of concrete elements with FRP strips is practical for reasons including: ease of installation, minimal disruption to functional integrity of the structure and low overall cost. FRP beam rehabilitation techniques are being refined and are subsequently becoming a viable rehabilitation method.

Data presented by many researchers[3,4,5] indicate that, with adequate bond strength and anchorage, application of a FRP strip to the tension face of a beam significantly increases capacity.   To design for beam rehabilitation it is fundamentally important that the expected increase in strength (capacity) and the change in ductile behaviour due to the application of the FRP strip are quantified. Steel reinforced concrete beams are traditionally designed to be under-reinforced to allow failure to be initiated by steel yielding, followed by considerable deformation at no substantial change in the load carrying capacity to ultimate failure by concrete crushing. This ductile behaviour is a desirable property as it provides warning of impending failure. When a FRP strip is bonded to an internally steel reinforced beam, a substantial change in the deformation behaviour can be expected due to increased reserve capacity at steel yielding. Recently, Duthinh and Starnes[5] presented an iterative numerical approach to predict the flexural strength enhancement and ductile behaviour change provided by FRP strip bonding of internally steel reinforced beams. Their approach involved iteration over two variables – the depth of the compression stress block and the concrete compressive strain at extreme fibres.

In this paper, a simple prediction method for estimating the flexural capacity and ductility behaviour of FRP reinforced beams is presented. The method involves iteration over only one variable – the concrete compressive strain at extreme fibres. The method is coded in MATLAB (Matrix Laboratory) and is verified by comparing the present results with those reported in the literature. Thereafter, the method is used to carry out a parametric study to investigate the influence of tensile steel reinforcement and composite reinforcement on the flexural and ductile behaviour of rehabilitated beams. Two types of composites, namely, carbon and glass fibre reinforced polymers are considered in the parametric study.

2. PREDICTION MODEL

For simplicity, the four point bending arrangement shown in Figure 1 is considered. This configuration generates tension along the bottom fibres of the beam – the fibres to which the FRP will be applied. The total beam length (L), the distance from the end of beam to load point (q) and the FRP bond length (L_{FRP}), are as defined in Figure 1.
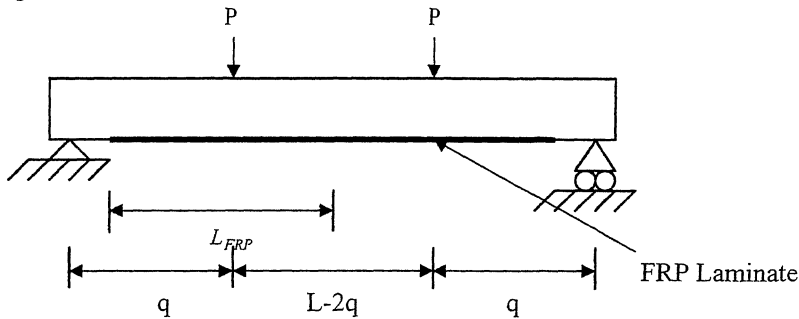

Figure 1: Four-point bending arrangement

Figure 2 shows the beam cross-section dimensions, reinforcement details, and strain and stress profiles across the depth of the beam. The beam considered here has tensile steel only. In developing the analytical model, we invoke Bernoulli's hypothesis of strain compatibility that plane sections remain plane, which requires perfect bonding between FRP and concrete. The stress-strain behaviour for steel was assumed to be linear elastic until steel yielding, and then perfectly plastic with a constant yield stress of f_{sy} in the post-yield region. The constitutive behaviour of concrete is represented by Hognestad's compressive stress parabola[6].
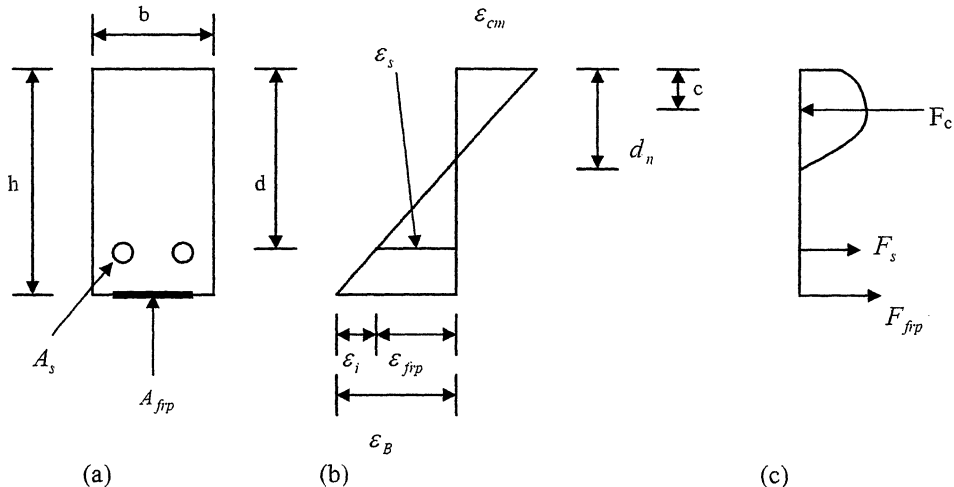

Figure 2: (a) cross section of beam, (b) strain diagram, and (c) force diagram

The model assumes beam failure by compressive concrete crushing at ultimate concrete strain[6], ε_{cu}, of 0.003. The key steps in the prediction algorithm are outlined below:

1. Determine ultimate moment capacity, M_v, of the virgin steel reinforced beam (ie. with no FRP) using the conventional rectangular stress block approach[6].

2. Choose the application (initial) moment, M_i. This value is a percentage of the virgin beam capacity. This moment represents the effects of existing loads at FRP application. For the purpose of this paper, the FRP is applied at a moment equivalent to 10% of the virgin beam capacity (except for the verification problems where values used in referenced sources are used).

3. Calculate the initial value of the extreme compressive and tensile fibre concrete strains, ε_{cmi} and ε_i, respectively, at FRP application.

4. Choose strain increment $\Delta\varepsilon = (\varepsilon_{cu} - \varepsilon_{cmi})/N$ where N is the total number of steps. A value of 20 has been used for N in this work. Then determine the current value of extreme compressive fibre concrete strain, $\varepsilon_{cm} = \varepsilon_{cmi} + (n-1)\Delta\varepsilon$ where n is the current step number. Using linear elastic stress-strain relations, express steel force, F_s, and FRP strip force, F_{frp}, in terms of the neutral axis depth, d_n, with Equations 1a and 1b. Express the resultant concrete force, F_c, by integrating Hognestad's concrete stress parabola[6] over the neutral axis to obtain Equation 1c.

$$F_s = A_s E_s \varepsilon_{cm} \left(\frac{d - d_n}{d_n} \right) \tag{1a}$$

$$F_{frp} = A_{frp} E_{frp} \left(\varepsilon_{cm} \left(\frac{h - d_n}{d_n} \right) - \varepsilon_i \right) \tag{1b}$$

$$F_c = b f_c' d_n \left(\frac{\varepsilon_{cm}}{\varepsilon_0} - \frac{\varepsilon_{cm}^2}{3\varepsilon_0^2} \right). \tag{1c}$$

Herein, E_s and E_{frp} denote Young's modulus of steel and FRP, respectively; and ε_o is the strain at which the concrete attains its compressive strength f_c'.

5. Determine the neutral axis depth, using the equilibrium condition:

$$F_c = F_s + F_{frp} \tag{2}$$

6. Determine FRP and steel strains, ε_{frp} and ε_s, respectively.

7. If $\varepsilon_B < \varepsilon_i$ or, $\varepsilon_{frp} > \varepsilon_{frpu}$; $F_{frp} = 0$. If $\varepsilon_s > \varepsilon_{sy}$; $F_s = A_s f_{sy}$. Herein, ε_{sy} and f_{sy} are, respectively strain and stress of steel at yield. ε_{frpu} is the ultimate tensile strain of FRP and let f_{frpu} denote ultimate strength.

8. If step 8 pertains to the analysis, amend the governing equilibrium equation by entering the new force values and solve for the neutral axis depth at the given compressive concrete strain.

9. Calculate depth, c, to the centroid of Hognestad's compressive stress parabola[6] as:

$$c = \frac{d_n (4\varepsilon_o - \varepsilon_{cm})}{4(3\varepsilon_o - \varepsilon_{cm})}. \tag{3}$$

10. Calculate the moment of resistance, M, and the mid-span curvature, ϕ_o as

$$M = F_s (d - c) + F_{frp} (h - c) \tag{4a}$$

$$\phi_o = \varepsilon_{cm} / d_n \tag{4b}$$

11. Increase the step number, n, by 1, and repeat steps 5 through 12 until n reaches the value N. The result of this will be a series of moment-curvature values. The moment-curvature values are used to determine the beam curvature distribution along the length.

12. Determine the central deflection, δ, by invoking the virtual work method. The following simplified expressions for δ are obtained by approximating the moment-curvature relationship by a bi-linear line:

$$\delta = \phi_o \left(\frac{L^2}{8} - \frac{q^2}{6} \right) \text{ for } \phi_o < \phi_y \tag{5a}$$

$$\delta = \frac{\phi_y}{6} q(p+q) + \frac{\phi_o}{24} \left[3L^2 - 4(p^2 + pq + q^2) \right] \text{ for } \phi_o > \phi_y, \tag{5b}$$

where $p = \left(\dfrac{M_y}{M} \right) q$; and M_y and ϕ_y are, respectively, moment and curvature at steel yielding.
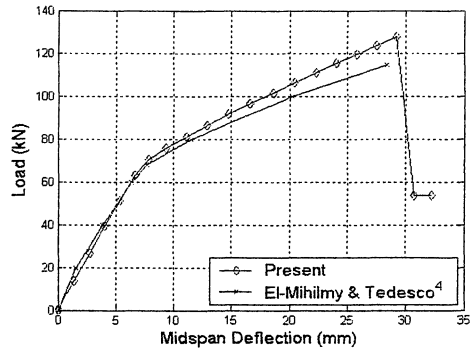
3. NUMERICAL RESULTS AND DISCUSSION

3.1 Model Verification

Results from the analytical model described in the previous section were compared with those available in the literature. For the purpose of this paper, FRP strip is assumed to be bonded over the full length of the beam. A comparison of present results with experimental moment-curvatures values for beam 4b in Duthinh and Starnes[5] are shown in Figure 3a. Figure 3b shows the comparison with experimental load-deflection results for beam b10 in El-Mihilmy and Tedesco[4]. It is noted that both beams are internally reinforced with steel and externally reinforced FRP. Beam dimensions, reinforcement areas and materials properties for these two beams are reported in Table 1.
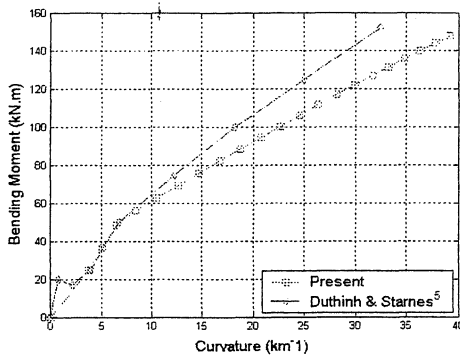
(a) Moment-curvature (beam 4b)   (b) Load-deflection (beam b10)

Figure 3: Comparison of moment-curvature and load-deflection results with other reported results

It should be noted that the model presented in this paper assumes that initial concrete cracking has occurred before application of the FRP laminate. Furthermore, experimental data from Refs 4 and 5 terminate at interfacial FRP/concrete failure. It can be seen from Figure 3 that present model results for moment-curvature are in reasonable agreement and those for load-deflection are in excellent agreement with experimental values reported in the literature. The error in moment capacity, expressed as a percentage of difference between present model results and experimental values relative to the experimental values, is 3.9% for Figure 3a and 11.3% for Figure 3b.

Table 1: Input data for comparison beams

Beam	b (mm)	H (mm)	d (mm)	A_s (mm^2)	f_{sy} (MPa)	A_{frp} (mm^2)	E_{frp} (GPa)	f_{frpu} (MPa)	f_c' (MPa)	L (mm)	q (mm)
Beam 4b	152	457	413	253	433	121.8	150	2400	42.7	2750	815
Beam b10	159	306	250	254	419	719	11.7	169	41.2	2438	914

3.2 Parametric Analysis

In this section, a parametric analysis using the proposed model is presented to show the influence of varying the cross-sectional area of tensile steel and FRP laminate for Carbon FRP (CFRP) and Glass FRP (GFRP). Table 2 gives numerical values of parameters that remained constant during the analysis.

Table 2: Constant beam parameters

FRP Type	B (mm)	H (mm)	D (mm)	f_{sy} (MPa)	E_{frp} (GPa)	f_{frpu} (MPa)	f_c' (MPa)	L (mm)	q (mm)
CFRP	150	460	415	400	150	2400	40	3000	1000
GFRP	150	460	415	400	12	170	40	3000	1000

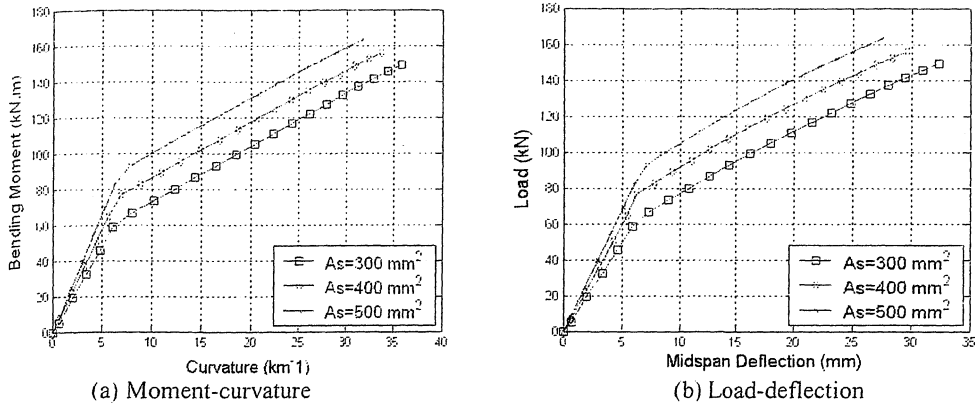(a) Moment-curvature   (b) Load-deflection

Figure 4: Moment-curvature and load-deflection relations for increasing steel area and a constant CFRP area of 121.8 mm^2.

For a constant CFRP area of 121.8 mm^2, moment-curvature and load-deflection relations for increasing values of steel area are shown in Figure 4.These moment-curvature plots suggest that moment capacity increases almost linearly with increasing tensile steel area. The load-deflection plots show that deflections reduce nearly linearly with increasing steel area for a given load. In other words, for a specified deflection, the load that can be resisted increases nearly linearly with increasing tensile steel area. Also, the plots suggest that load-deflection form does not change with increasing steel area. After steel yielding, lines corresponding to different steel areas are parallel. This can be attributed to tensile stress redistribution to the tensile steel. Since it has been assumed that tensile steel is perfectly plastic after the yield point, the moment-curvature and load-deflection relations can be expected to be parallel in the nonlinear stress range.

Moment-curvature and load-deflection plots for a constant steel area of 253 mm^2 and for increasing values of CFRP area are presented in Figure 5. Model predictions for beams rehabilitated with GFRP are shown in Figure 6. In Figures 5 and 6, the lines corresponding to FRP area of zero belong to conventional steel reinforced beams (i.e. beams with no FRP).
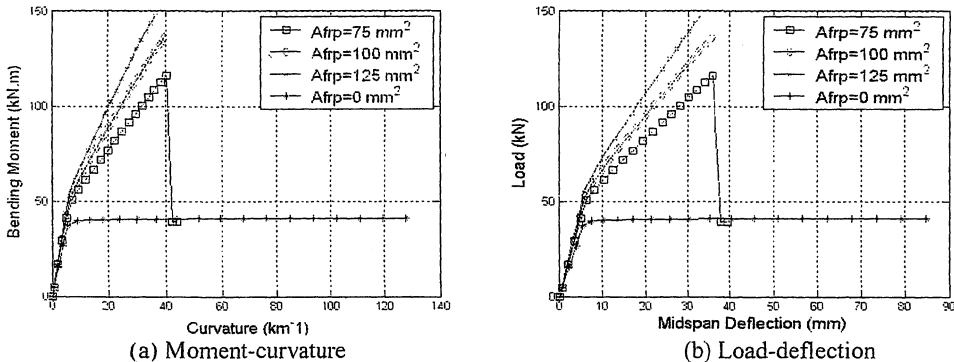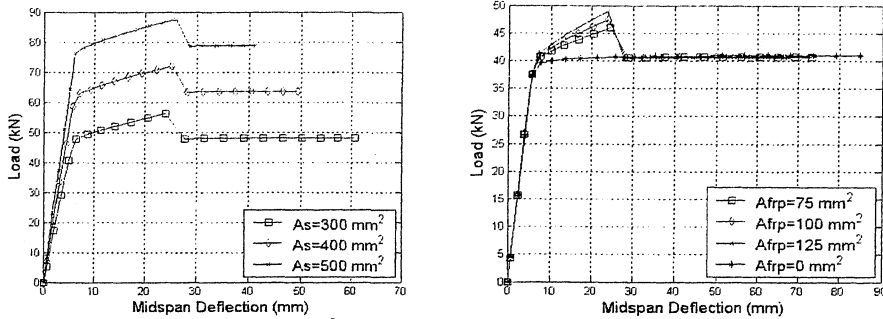

(a) Moment-curvature   (b) Load-deflection

Figure 5: Moment-curvature and load-deflection relations for increasing CFRP area and a constant steel area of 253 mm^2.

Figures 5 and 6 provide valuable qualitative information about the mechanics of FRP-rehabilitated RC beams. They clearly illustrate the increased moment resistance ability of these beams, relative to conventional beams. The effect of varying FRP area and type seems ineffective in the linear elastic range. However, in the non-linear range, the effect of varying FRP area and type becomes significant. Figures 5 and 6 suggest that increased FRP area increases section stiffness (i.e. reduces deflection) at different rates. But this only occurs in the nonlinear region. This can be attributed to load redistribution inside the section (see figure 2 (c)) following steel yielding. A comparison between Figures 5(b) and 6(b) shows that CFRP reinforced beams have much lower mid-span deflections than that for GFRP reinforced beams for the same load. This is mainly due to high stiffness of CFRP in comparison to GFRP. The reduced strength characteristics of GFRP, relative to CFRP, are indicated by comparison between Figures 5 and 6. Figure 6

565

shows that, following FRP tensile rupture, the load-deflection and moment-curvature relations instantaneously reduce to that of a conventional RC beam, without FRP-rehabilitation.

(a) For a constant FRP area of 121.8 mm²   (b) For a constant steel area of 253 mm²

Figure 6: Load-deflection relations for beams rehabilitated with GFRP.

4. CONCLUSION

A simple analytical model that predicts the moment-curvature and load-deflection relations for concrete beams reinforced with internal steel and external FRP composite materials has been presented. The study is limited to a four-point bending arrangement of the beam in the present work. The model results have been verified by comparing with reported results in the literature. The results of a parametric analysis showing the influence of varying amount of steel and composite reinforcement are presented. The following conclusions can be drawn:

1. The addition of a FRP laminate strip to the tension face of a reinforced concrete beam considerably increases sectional capacity.
2. Simple equilibrium mechanics can be employed to quantify the linear elastic and nonlinear plastic load-deflection and moment-curvature relationship.
3. The stiffness of a FRP/concrete beam is not enhanced with type of FRP or additional FRP area in the linear elastic range.
4. Changing the FRP material type induces behavioural changes of the beam. Section stiffness increases with increasing FRP elastic modulus.
5. Section stiffness increases with FRP area - this is ostensible in the nonlinear range.

It should be noted that this study has assumed the failure of FRP reinforced concrete beam as concrete crushing at extreme compressive fibres. However, there is growing evidence that failure happens by debonding near the FRP/concrete interface before concrete crushing at extreme compressive fibres. The authors are currently investigating how to accommodate this failure mode into the simple analytical model presented here.

REFERENCES

[1] M. Tavakkolizadeh and H. Saadatmanesh, 'Repair of damaged steel-concrete composite girders using carbon fiber-reinforced polymer sheets', *Journal of Composites for Construction*, ASCE, **7(4)**, pp. 311-322, 2003.

[2] U. Meier, 'Bridge repair with high performance composite materials', Mater. Tech. (Duebendorf, Switz.), **15**, pp. 125-128, 1987.

[3] M. Arduini, A. D. Tommaso and A. Nanni, 'Brittle failure in FRP plate and sheet bonded beams', *Structural Journal*, ACI, **94(4)**, pp. 363-370, 1997.

[4] M. T. El-Mihilmy and J.W. Tedesco, 'Deflection of reinforced concrete beams strengthened with fibre-reinforced polymer (FRP) plates', *Structural Journal*, ACI, **97(5)**, pp. 679-688.

[5] D.Duthinh and M. Starnes, 'Strength and ductility prediction of concrete beams reinforced with carbon fiber-reinforced polymers plates and steel', *Journal of Composites for Construction*, ASCE, **8(1)**, pp. 59-69, 2004.

[6] R.F. Warner, B.V. Rangan, A.S. Hall and K.A. Faulkes, *Concrete Structures*, Longman, Melbourne, 1999.